European Journal of Pharmaceutics and Biopharmaceutics 72 (2009) 418–427

Contents lists available at ScienceDirect

European Journal of Pharmaceutics and Biopharmaceutics

journal homepage: www.elsevier.com/locate/ejpb

Research paper

Functionalized nanospheres loaded with anti-angiogenic drugs: Cellular uptake and angiosuppressive efficacy

Taha Hammady, Jean-Michel Rabanel, Renu Singh Dhanikula, Grégoire Leclair, Patrice Hildgen *,[1]

Faculté de pharmacie, Université de Montréal, Montréal Que., Canada

ARTICLE INFO

Article history:
Received 5 August 2008
Accepted in revised form 16 January 2009
Available online 25 January 2009

Keywords:
Functionalized nanospheres
Co-encapsulation
Internalization
HUVECs
Rat aortic ring
Angiogenesis
Selectin
Paclitaxel
Endostatin

ABSTRACT

The objective of this study was to develop polymeric nanospheres (NPs) that are able to selectively target the activated vascular endothelium and to deliver co-encapsulated anti-angiogenic agents for improved treatment efficacy in inflammatory diseases with an angiogenic component. We evaluated a novel poly(D,L)-lactide (PLA)-based polymer, grafted with a synthetic ligand specific for selectin ($PLA^{-g\text{-}SEL}$), for the preparation of functionalized NPs. The NPs were produced according to a double emulsion–solvent diffusion/evaporation method, allowing the co-encapsulation of hydrophilic and lipophilic drugs.

Incorporation of the functionalized polymer enhanced the internalization of fluorescein-labeled NPs by lipopolysaccharide-activated vascular endothelial cells relative to control NPs, as evidenced by confocal laser scanning microscopy and quantitative fluorescence measurements. Two anti-angiogenic agents, endostatin and paclitaxel, were co-loaded in the functionalized NPs. Respective drug loadings were optimized by adjusting polymer composition, as well as by the microemulsion technique.

NPs loaded with either of the chosen drugs or with a combination of them were tested for their anti-angiogenic efficacy in human umbilical vascular endothelial cell (HUVEC) culture *in vitro* and rat aorta tissue culture *ex vivo* models. An enhanced anti-proliferative effect on HUVECs and heightened anti-angiogenic action on rat aorta ring cultures was observed for the loaded drugs compared to the free molecules. Moreover, combined loaded treatments were found to be more potent, evoking additive and even synergetic outcomes (at lower doses) greater than the corresponding single-loaded treatments in inhibiting new vessels sprouting in rat aortic rings.

1. Introduction

In the recent decades, the process of pathological angiogenesis has become the focus of interest in many research laboratories [1]. This can be easily understood by virtue of the evident contribution of such processes in many serious diseases, such as solid tumors, arthritis, psoriasis, diabetic retinopathy and atherosclerosis [2]. Angiogenic inhibitors have been approved for the treatment of cancer in the USA and European Union, nevertheless, malignant tumors have been shown to develop resistance to anti-angiogenic monotherapy by producing redundant angiogenic factors that are not matched by the inhibitors used [3]. In this respect, it has been demonstrated that the combination of angiogenesis inhibitors can broaden their therapeutic efficiency and could be very valuable in preventing refractory states of cancer [4,5].

Many inhibitors have been investigated, from hydrophilic peptidic endogenous regulators to hydrophobic chemotherapeutic agents, and some of them have already reached clinical trials. For example, endostatin (EN) is a COOH– terminal fragment of collagen XVIII, consisting of 184 amino acids. It was initially isolated from the conditioned medium of hemangioendothelioma cells [6]. EN represents a broad-spectrum angiogenesis inhibitor, since it targets angiogenesis regulatory genes on more than 12% of the human genome [7]. Perhaps the most interesting features of EN are the lack of side-effects, and no acquired resistance is induced by its prolonged administration [8]. However, systemic delivery of recombinant EN raises a number of problems, such as its short half-life *in vivo* and the need for long-term treatment whether continuous or intermittent [9]. Therefore, the design of an appropriate drug delivery system would be worthwhile for the development of successful therapy.

On the other hand, a number of chemotherapeutic agents have recently been studied for their anti-angiogenic activity. Paclitaxel (PX) is considered to be one of the most outstanding candidates to join the arsenal of anti-angiogenic drugs [10,11]. At lower doses than those required for cytotoxic effects, PX has been shown to inhibit tumor growth by suppressing the expression of basic growth

* Corresponding author. Faculté de pharmacie, Université de Montréal, C.P. 6128, Succursale Centre-ville, Montreal, Que., Canada H3C 3J7. Tel.: +1 514 343 6448; fax: +1 514 343 6871.
E-mail address: Patrice.hildgen@umontreal.ca (P. Hildgen).
[1] Co-director of the "Groupe de Recherche Universitaire sur le Médicament", Université de Montréal (Research group supported by Fonds de la recherche en santé du Québec – FRSQ).

0939-6411/$ - see front matter © 2009 Elsevier B.V. All rights reserved.
doi:10.1016/j.ejpb.2009.01.007

factor and vascular endothelial growth factor [10,12]. However, PX delivery is hampered by its poor water solubility, resulting in the use of Cremophor®, an adjuvant responsible for serious adverse effects. Thus, many groups have attempted to increase PX's therapeutic efficacy and to reduce its systemic side-effects through microencapsulation in polymeric nanospheres (NPs) [12–14].

Pathological angiogenesis is always associated with acute or chronic inflammation, with specific receptors being overexpressed by the vascular endothelium [15]. For instance, E-selectin is a surface membrane receptor upregulated in many disease conditions characterized by inflammation and recruitment of leukocytes, including malignant tumors and their metastases, arthritis, inflammatory bowel disease, psoriasis and dermatitis [16]. Therefore, we hypothesized that NPs made from a polyester-based, ligand-grafted polymer [17], that can specifically adhere to the endothelium overexpressing selectins, could be valuable by targeting anti-angiogenic treatment towards the pathological vasculature. In fact, NPs prepared from biodegradable polyesters are an attractive tool to achieve this goal; besides active targeting, polymeric NPs prepared by the double emulsion-solvent diffusion/evaporation method may allow the co-encapsulation of lipophilic and hydrophilic therapeutic molecules [18,19]. Regarding the NPs targeting capabilities, we choose as the targeting ligand, a synthetic analog of Sialyl Lewis^x that has been shown to be specific for E- and P-selectins [20].

The aim of this work was to optimize the co-encapsulation of two anti-angiogenic molecules with distinct physicochemical features interfering on different pathways, to obtain a highly effective anti-angiogenic treatment. EN, a hydrosoluble peptide, was loaded in the aqueous phase of w/o/w NPs, whereas PX was incorporated in the polymeric matrix. Thus, NPs loaded with either EN or PX or both were produced according to the solvent diffusion/evaporation method with the objective of optimizing their respective encapsulation efficiencies (EEs). The selective cellular uptake of NPs prepared, using poly(D,L)-lactide-based polymer grafted with a selectin-specific ligand (PLA$^{-g\text{-}SEL}$), was investigated in human umbilical vascular endothelial cell (HUVEC) cultures. Finally, the anti-angiogenic efficacy of NPs loaded with either EN or PX (or both) was assessed *in vitro* by quantifying the proliferation of HUVECs via their enzymatic activity and *ex vivo* in a tissue culture model, rat aortic rings. The latter model allows the monitoring of tubule formation as an angiogenesis index over a long period of time.

2. Materials and methods

2.1. Materials

PX was a kind gift from BioexelPharma Inc. (Saint-foy, Que., Canada), whereas mouse EN was purchased from EMD Biosciences (San Diego, CA, USA). Mouse endostatin EIA kits were procured from Cytimmune (Rockville, MD, USA). The murine macrophage cell lines Raw 264.7 and Huvec-ec (CRL1730) were from the American Type Culture Collection (ATCC, Manassas, VA, USA), and cell culture media were from Gibco (Invitrogen, Burlington, Ont., Canada). All reagents were from Sigma–Aldrich (St.-Louis, MO, USA), whereas reagent-grade solvents were from Laboratoire MAT (Montreal, Que., Canada).

2.2. Ligand and polymer synthesis

The selectin ligand (SEL) was synthesized and grafted on polyester-based polymer in the laboratory, as described previously [21]. Briefly, PLA$^{-g\text{-}SEL}$ was synthesized from PLA functionalized with 1% pendant acid chloride groups [17]. Grafting was then achieved through the reaction of this active pendant group with an unprotected non-essential hydroxyl group on the ligand molecule. Finally, hydroxyl groups of the ligand moiety were de-protected by catalytic hydrogenation, and the polymer obtained was freeze-dried. The molecular weight (M_w) of the polymer was found to be 40,791 Daltons (Da), as determined by size exclusion chromatography (SEC). Similarly, fluorescein molecules were grafted on the same functionalized PLA to yield PLA$^{-g\text{-}FLU}$ by reacting the hydroxy group of fluorescein with pendant acid chloride group. Unreacted fluoresceins were eliminated by repeated polymer precipitations in water, and the fluorescent polymer was freeze-dried until further use.

PLA was prepared by the ring-opening polymerization of dilactide under argon atmosphere, employing tetraphenyl tin as catalyst. The multiblock co-polymer of poly(D,L)-lactide and poly(ethyleneglycol) (PLA-PEG-PLA)$_n$ was synthesized according to Quesnel and Hildgen [22]. The respective M_ws were found by SEC to be 50,000 Da for PLA and 16,000 Da for the multiblock co-polymer. Commercial poly(lactide-co-glycolide) (PLGA, Resomer® RG504), M_w 48,000 Da, was from Boehringer-Ingelheim (Ingelheim am Rhein, Germany).

2.3. Polymer cytocompatibility studies

Raw 264.7 cells were cultured in Dulbecco's Modified Eagle Medium (DMEM) supplemented with 10% fetal bovine serum (FBS) and penicillin/streptomycin (Invitrogen, Burlington, Ont., Canada). The cells were grown in tissue culture flasks and incubated at 37 °C in 5% carbon dioxide atmosphere.

2.3.1. Proliferation assay

Polymers dissolved in 10 μl dimethyl sulfoxide (DMSO) were added in 96-well flat-bottomed microplates (Corning Inc., Corning, NY, USA), in triplicate. The amounts tested were 250, 100, 10, 1, 0.1 and 0.01 μg. DMSO was subsequently removed under vacuum. The Raw 264.7 cells were diluted in complete medium at a final concentration of 5×10^5 cells/ml and plated (100 μl/well). The plates were incubated for 24 h, after which cell proliferation was assessed by MTT assay [23]. Briefly, 10 μl of thiazolyl blue tetrazolium bromide (Sigma, St.-Louis, MO, USA), dissolved in phosphate-buffered saline (PBS, (10 mM, pH 7.4) at a concentration of 5 mg/ml and filtered on 0.22 μm sterile filter (Millipore, Bedford, MA, USA), was added to each well. After 3-h incubation time at 37 °C in 5% carbon dioxide atmosphere, 50 μl of a lysing solution (Isopropanol, 10% Triton X-100, 0.1 N HCl) was added to each well to dissolve the dark blue formazan crystals. Absorbance was read at a 570 nm wavelength on a microplate reader (SAFIRE®, Tecan, Austria).

2.3.2. Lysis assay

The presence of lactate dehydrogenase (LDH) in supernatants from proliferation assays served as an indicator of cell lysis and cytotoxicity. It was quantitated with commercial dosing kits (Sigma, St.-Louis, MO, USA), as directed by the manufacturer. Briefly, after 24-h incubation of Raw 264.7 cells in the presence of the tested material, 5 μl of cell supernatants was transferred to new microplates and incubated in the dark with the reaction mixture for 30 min. The reaction was stopped with 0.1 N HCl. The microplates were read by microplate reader, at 450 nm wavelength (reference wavelength 690 nm). The results are plotted in reference to positive control wells, 100% Triton X-100 lysed cells.

2.4. Preparation of NPs

2.4.1. Drug-loaded NPs

All NPs were prepared according to an adjusted double emulsion-solvent diffusion/evaporation technique [24,25]. Briefly, the

organic phase consists of 0.25 g of the polymer (or polymer blend) plus 0.125, 1.25, or 12.5 mg of the lipophilic ingredient PX, dissolved in 10 ml dichloromethane (DCM). The organic phase incorporated variable amounts of Span 80, as described previously [25], and was associated with *n*-butanol as co-surfactant in certain batches (see Table 2 for quantities). The w/o/w double emulsion was prepared by a 2-step emulsification procedure. First, different quantities of the hydrosoluble peptide EN (250, 500, or 1000 μg) were dissolved in 250 μl of citrate-phosphate buffer, pH 6.2. The w/o primary emulsion was then obtained by dispersing EN aqueous solution in the previously described organic phase, by vortexing for 1 min, followed by 15 s homogenization with a high-speed turbo stirrer. The primary w/o emulsion was then gently syringed into 100 ml of 15% w/v sucrose aqueous solution containing a surfactant mixture (2.5% Tween 20/0.5% PEG oleate), while emulsification was being achieved by means of high-pressure homogenization with Emulsiflex C30 (Avestin, Ottawa, Ont., Canada) at 10,000 psi for 3 min to generate a multiple w/o/w emulsion. The latter was collected, and its volume was adjusted to 250–300 ml with the external aqueous phase. Finally, it was stirred for 3 h under reduced pressure to allow extraction of the volatile organic solvent and, hence, the subsequent solidification of NPs. Batches containing either EN or PX were prepared by the same procedure, except for omitting either EN in the aqueous phase or PX in the organic phase. Batch names along with the formulation parameters of each batch are presented in Table 1.

2.4.2. Fluorescein-labeled NPs

For targeting studies, blank NPs were prepared according to the above-mentioned procedure where citrate-phosphate buffer, pH 6.2, was used as the internal aqueous phase of the w/o/w emulsion. Fluorescein labeling of blank NPs was achieved by blending in DCM fluorescein-labeled PLA ($PLA^{-g\text{-}FLU}$) with the other polymer(s) in a ratio of 1:3 (w/w) for all batches, before the double emulsion (Table 3).

2.4.3. Recovery of NPs

Freshly prepared NP dispersions were purified and concentrated according to a modified diafiltration technique, as reported previously [25]. Complete removal of surfactants was monitored during the course of the diafiltration by measuring surface tension using a Surface Tensiomat®21 (Fisher Scientific, Ottawa, Ont., Canada). NP concentrates were aliquoted and conserved at −20 °C. For characterization purposes, a fraction of each drug-loaded batch was recovered and washed by conventional ultracentrifugation/re-dispersion cycles. Finally, NPs were dispersed in deionized water, freeze-dried, and stored at −20 °C for subsequent investigation.

2.5. Determination of EEs and loading

Ten milligrams of lyophilized NPs were weighed in a sterile vial, and re-dispersed in 3 ml PBS, pH 7.4. The dispersed NPs were then degraded with 2 ml chloroform, and extraction was facilitated by rotating the vials end-over-end in a rotating plate for 6 h at ambient temperature. The samples were then centrifuged at 14,000 rpm for 5 min, and 1000 μl of the aqueous supernatant was drawn off by micro-tipped pipette. EN was assessed in the aqueous layer by enzyme immunoassay (Mouse Endostatin Competitive EIA kit, Accucyte®), following the manufacturer's instructions. EE was calculated as drug percentages in NPs relative to the initial amount: EE = Drug in NPs/Initial amount × 100.

The PX fraction extracted in the aqueous layer was analyzed by the first-derivative spectrophotometry at 240 nm, and its concentration was quantitated with reference to a standard calibration curve. To assess PX content in the organic layer, 0.5 ml of the chloroform layer was mixed with 10 ml ethanol to precipitate the polymer. After centrifugation, PX concentration was determined by spectrophotometry in supernatant alcoholic solution as mentioned above. PX determination was done by measuring the valley amplitude at λ = 240 nm in the first-derivative curve. The linear range of detection was found to be between 0.25 and 0.5 μg/ml. Total PX EE was calculated as follows: $PX_{total} = [PX_{aqueous\ phase} + PX_{organic\ phase}]/\text{Initial amount} \times 100$.

Table 1
Formula names of NP batches according to their variable manufacturing parameters.

Formula name	Polymer ratio (per weight)			Co-surfactant (% v/v)[a]
	$PLA^{-g\text{-}SEL}$	PLA	Multiblock	*n*-Butanol
PLA-*S*	1	1	–	–
BuPL-*S*	1	1	–	16.6
MuPL-*S*	2	1	1	–
BMPL-*S*	2	1	1	16.6

[a] *n*-Butanol volume was calculated on the basis of total volume of the organic phase in the w/o primary emulsion.

2.6. Determination of particle size and zeta potential of NPs

NP particle sizes were measured by photon correlation spectroscopy (PCS) in a N4Plus Coulter Nanosizer (Coulter Electronics, Miami, FL, USA). Measurements were taken at 25 °C with a scattering angle of 90°, and the mean (±SD) of at least three readings was calculated. Moreover, zeta potential of the NPs was analyzed by at least three consecutive readings of sonicated NP dispersion in 0.22-μm filtered, diluted PBS, with a zeta potential analyzer (Zetasizer Nanoseries, Malvern Instruments, Worcestershire, UK).

2.7. Uptake of NPs by HUVECs

2.7.1. Cell culture

HUVECs (ATCC, cell line CRL1730) were grown in F-12 Kaighn modification medium supplemented with 15% FBS, 100 μg/ml penicillin/streptomycin, 300 μg/ml endothelial cell growth supplement (ECGS), and 120 μg/ml heparin (Sigma, St.-Louis, MO, USA). The medium was renewed every 3 days until 70% confluency.

2.7.2. Qualitative study

Glass cover slips were sterilized and mounted in 24-well culture plates. HUVECs were then seeded in the wells at 2×10^3 cells per well. To enhance cell attachment, coverslips were pre-treated with a 10 μg/ml fibronectin solution (Chemicon, Millipore, Bedford, MA, USA). The culture was incubated at 37 °C for 48 h. After renewal of the nutrient medium and 4-h induction with LPS (lipopolysaccharide from *Escherichia coli*), the uptake of fluorescein-labeled NPs was initiated by exchanging the medium with a NP dispersion adjusted to the same tonicity of the culture medium by lyophilized F-12 Kaighn medium. The final concentration of NPs was 100 μg/ml. The culture was then re-incubated for 12 h. At fixed time intervals, the experiment was stopped in pre-selected wells by discarding NPs containing medium and washing 3–4 times with pre-warmed Hank's balanced salt solution (HBSS) to eliminate excess unbound particles.

Specimens were prepared for confocal laser scanning microscopy by fixing the cells with 4% formaldehyde in HBSS solution. Cover slips were then mounted on glass slides with GelTol® mounting medium (Thermo Electron Corporation, Waltham, MA, USA). The samples were finally kept at 4 °C until subsequent examination. Confocal laser scanning microscope images were acquired at 40× and 100×, with a Leica TCS SP2 confocal system (Leica Microsystems, Heidelberg, Germany), using FITC filters (λexc. 495 nm, λem. 510 nm). All images were processed with ImagePro® software (MediaCybernetics, Bethesda, MD, USA).

2.7.3. Quantitative studies

The experiments in this section were conducted in 75 cm^2 culture flasks. HUVECs were allowed to proliferate to 70% confluence. Medium was substituted by complete growth medium premixed with 1 ml of NP dispersion with adjusted tonicity as mentioned above (NP final concentration 100 μg/ml). The tested cultures were further incubated for 12 h. To end the experiment, the medium was removed and the cell monolayer was washed three times with HBSS to eliminate excess particles. Afterwards, the cells were detached from the bottom of the flask with a sterile scraper, and transferred to sterile tubes, then precipitated by centrifugation at 1500 rpm for 10 min. The cell pellet and the uptaken NPs were lysed with lysing solution (0.25% Triton X-100 in 1 N NaOH). Fluorescence was assessed by spectrofluorometry (λexc. 488 nm, λem. 530 nm), and an equivalent amount of fluorescein was calculated with reference to a fluorescein standard calibration curve. NP fluorescein content was quantitated by spectrofluorometry, by dissolving 10 mg of NPs in NaOH/Triton X-100 and by comparing the value obtained with a fluorescein calibration curve in the same medium. Fluorescence measurements were normalized with total protein content quantitated with BCA protein assay kits (Pierce, Rockford, IL, USA), according to the manufacturer's instructions.

2.8. Validation of anti-angiogenic activity

2.8.1. HUVEC proliferation assay

To assess the effects of free drugs, blank and drug-loaded NPs on endothelial cell proliferation, MTT assays were performed on HUVECs cultured on 96-well plates at 2×10^3 cells/well. After overnight incubation, the medium was renewed and LPS (5 μg/ml) was added. After 4-h incubation, aliquots of the free drug, blank or drug-loaded NP dispersions (NP dispersions isotonic with culture medium) were added to the wells and incubated for 72 h. The assay was replicated eight times for each treatment tested. Endothelial cell viability and cell growth in vitro were quantitated by colorimetric MTT assay, as described in Section 2.3.1 [23].

2.8.2. Rat aortic ring assays

An established tissue culture model involving rat aortic rings was adapted for our purposes [26]. First, 24-well culture plates were pre-coated with collagen gel, which had been prepared by quickly mixing rat-tail collagen solution (3 mg/ml) prepared according to [27]_and DMEM with glutamine, supplemented with 7% fetal calf serum and 0.1 N sodium hydroxide (6:7.5:1 v/v) at 4 °C. Each well was coated with 0.5 ml of the mix, and gelation was allowed for 1 h at 37 °C. After removing fibro-adipose tissues, 1-mm thick rings of cleaned aorta were washed in sterile HBSS, and then carefully placed in the collagen pre-coated wells. Aliquots of the tested preparation (either free drug solution, blank or drug-loaded NP dispersions normalized with lyophilized culture medium, as explained above, or controls) were deposited on the center of each aortic ring. Control wells were treated with blank conditioned medium solution with or without blank functionalized NPs. These 24-well plates were incubated at 37 °C for 20 min, followed by the application of the second layer of the collagen mixture on each well. After gelation, 0.5 ml of enriched medium consisting of supplemented DMEM, ECGS (15 mg/ml), epidermal growth factor (10 ng/ml), and insulin (5 μg/ml) was added to the wells and the culture was incubated at 37 °C in 5% carbon dioxide atmosphere.

Photos of the embedded artery rings were captured on the 7th and 14th days of culture, by Canon PowerShot A95 digital camera (Canon, Canada) with an Axiovert S100 inverted microscope under 40× magnification (Zeiss, Oberkochen, Germany). The images were then processed for the quantification of new tubules and their ramifications by photo binarization to black/white, according to the visual inspection of vascular morphology [28] with PaintShop Pro® software. Vascular density was quantitated by Optimas7® image analysis software and expressed as percentages of blackened tubules relative to the whitened background (see Fig. 5). Four images per well ($n = 3$) and condition were analyzed. Finally, the data were normalized with those of positive control wells for each plate, to reduce plate to plate variability.

2.9. Statistical and drug effect analyses

Quantitative data were calculated as means ± SD. Statistical analysis of HUVEC proliferation assays and rat aortic ring assays was achieved by one-way ANOVA after testing for normality and equality of variances. Data were analyzed by Fisher's lower significance difference (LSD) test with Sigmastat 3.0 (Systat Software, CA, USA). Differences were considered significant when $p < 0.05$. *T*-test was performed to determine the statistical significance of putative additive or synergetic effects of multiple drug treatments. Significance was established by pairing the results of multiple drug treatments with data on single drug exposures under the same conditions and doses.

3. Results and discussion

3.1. Cytocompatibility of $PLA^{-g\text{-}SEL}$

The cytocompatibility of two different batches of the synthesized polymer was assessed, as described in the experimental section on the Raw 264.7 cell line. MTT colorimetry was undertaken to quantitate enzymatic activity as an index of cell proliferation, since it measures the tetrazolium ring cleavage by the active mitochondria of living cells [23]. Besides, LDH levels in culture supernatants indicate the extent of cell lysis. MTT assay demonstrated no effect on cell proliferation with the polymer batches tested in the 0.1 to 1000 μg/ml concentration range (Fig. 1A). Moreover, LDH assay revealed no significant cell death (Fig. 1B). The results obtained were comparable to those from the parallel assessment of a standard sample of FDA-approved poly(lactide-co-glycolide) co-polymer (Resomer® RG504, Boehringer-Ingelheim). Similarly, the other polymers employed in the preparation of NPs were tested and showed no toxicity in the same concentration range [29].

3.2. Encapsulation efficiencies

Efforts, undertaken in the field of microencapsulation of hydrosoluble macromolecules, such as proteins, peptides, and DNA plasmid, in polymeric NPs, have led to many strategies for improved loading. For example, polymer blends represent one of the most interesting approaches to enhance protein loading. A polyester polymer can be mixed with a more hydrophilic PEGylated co-polymer or polymeric surfactant to improve protein affinity for the polymeric matrix. Sanchez et al. suggested a PLGA/poloxamer blend to improve the loading recovery of interferon alpha [30]. Alternatively, the incorporation of some stabilizing agents, such as bovine serum albumin or a non-ionic surfactant in the inner aqueous layer, has also been valuable in increasing the loading efficiency and stability of microencapsulated proteins [31,32].

In the previous work, we demonstrated that the microemulsion technique could significantly improve the EE of a hydrosoluble macromolecule model [25]. Coupling this technique with the incorporation of a PEGylated co-polymer, such as $(PLA\text{-}PEG\text{-}PLA)_n$, has further enhanced the loading values. Yet, the issue should be re-considered in cases of co-encapsulation of a lipophilic agent with a hydrophilic macromolecule. It has been observed that the above-mentioned techniques, aiming to enhance the loading of

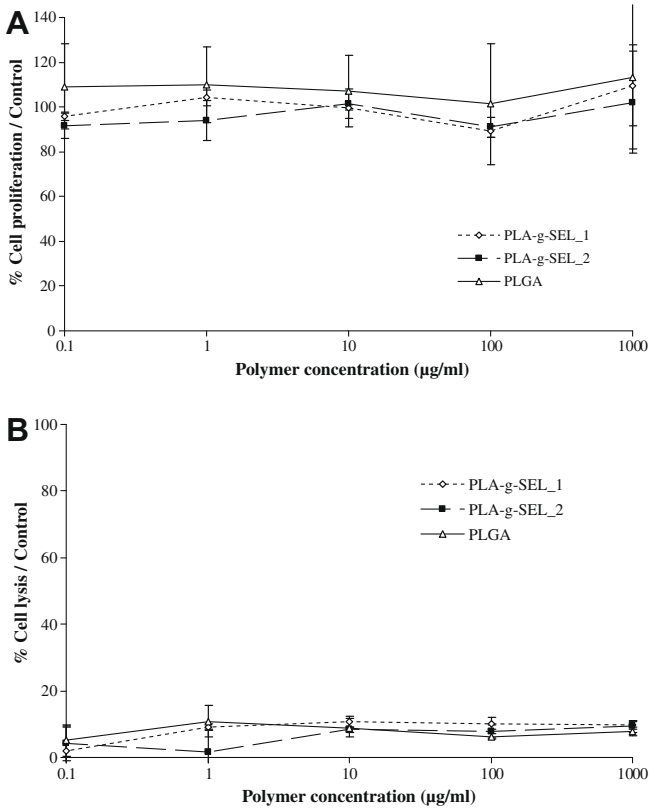

Fig. 1. Polymer cytocompatibility assays. (A). MTT assays on Raw 264.7 cells for two prepared batches of the ligand-grafted polymer PLA$^{-g\text{-}SEL}$. Standard PLGA is used as reference. (B). LDH assays on Raw 264.7 cells for two prepared batches of the ligand-grafted polymer PLA$^{-g\text{-}SEL}$. Standard PLGA is used as reference.

hydrophilic agents, usually have a negative impact on the loading of poorly water-soluble drugs [19,33]. Hence, in the current work, we tried to achieve optimal balance in loading efficiency between the two anti-angiogenic drugs, knowing that EN as a protein is one of the most difficult molecules to encapsulate, while the EE of PX in polyester NPs can reach 100% [34].

Both the microemulsion technique (addition of Span 80/*n*-butanol) and the incorporation of PEG-PLA multiblock co-polymer raised the EE of EN compared to standard conditions (Table 2). Nevertheless, as expected, the PX-loading rate was reduced by both the approaches, with a more pronounced effect associated with *n*-butanol incorporation. Moreover, the combination of both techniques further raised the EE of EN to 71.3%, whereas the EE of PX was reduced to 56.8% (batch 4). The hydrophilic contribution of PEG-PLA multiblock co-polymer (limited to 25% of polymer weight) appeared to be responsible for the slight decrease in PX loading as a consequence of its reduced affinity for the polymeric matrix. On the other hand, the partially water-miscible solvent *n*-butanol, as co-surfactant, seemed to facilitate PX diffusion into the external aqueous phase during preparation of the double emulsion. Such events could also account for significant depression of its EE (Table 2). As expected, coupling of the two techniques resulted in a kind of double-headed additive effect that enhanced EN retention from one side, and decreased that of PX from the other side. As a consequence, batch 4 (Table 2), showing the highest EN-loading along with fair PX loading, was retained for further efficacy assays.

3.3. Particle size distribution and zeta potential

Particle size data analysis revealed that all batches were in the nanometric (200–250 nm) range without wide variations between batches (Table 2). Moreover, the values were consistent with those observed in a previous work [25]. This means that the surfactant blend (here Tween 20/PEG oleate) could successfully substitute for PVA as the stabilizer of the secondary emulsion [35]. PVA, due to its suspected carcinogenic and cytotoxic effects, should be avoided in the parenteral applications [35], while the group of non-ionic surfactants such as Tween (polyoxyethylene-based surfactants) is acceptable [36]. On the other hand, it is noteworthy that the enhancement of EN-loading efficiency was accompanied by a slight increase in the mean particle size of the loaded NPs (Table 2). Since the peptide was incorporated as an aqueous buffer solution, such a finding could be explained by the higher retention of this solution in the NP matrix, which, in turn, reflects the enhanced stability of the primary emulsion. No effect of PX loading has been observed on NP size.

Zeta potential is an important index of NP surface charge in aqueous dispersions. High electric charge on surface-loaded NPs ensures enough repellent forces among particles and prevents their aggregation [37]. All prepared batches were found to be negatively charged, with an average value of −24.5 mV for NPs made from PLA/PLA$^{-g\text{-}SEL}$ polymer blend (Table 2). However, the (PLA-PEG-PLA)$_n$ co-polymer in NP preparations induced a decrease in their zeta potential which moved to an average value of −10.0 mV due to the presence of PEG moieties at the NP surface.

The clearance of surfactants in NP preparations was tracked by surface tension measurement using a standard tensiometer. The dialysis was continued until the surface tension of the dispersion solution has been raised to approach that of deionized water (data not shown).

3.4. NP uptake by HUVECs

NP uptake was studied with blank NPs (without loaded drugs), prepared according to the same procedures as for drug-loaded NPs. Particle size and zeta potential data on blank, fluorescein-labeled NPs used in uptake experiments are tabulated along with their polymer blend compositions in Table 3. The particle size values obtained were in good accordance with those depicted earlier in Table 2 for drug-loaded NPs. Four hours before the start of either the

Table 2
Characteristics of drug-loaded NP formulations. NPs were co-loaded with 2 µg/mg polymer of endostatin (EN), and 50 µg/mg polymer of paclitaxel (PX) was prepared by the double emulsion-solvent evaporation method (means ± SD, $n = 3$).

Batch No.	Formula name	EN loading	% EE for EN	PX loading	% EE for PX	Mean diameter (nm)	Zeta (mV)
1	PLA-*S*	0.53 ± 0.05	26.4 ± 2.7	39.91 ± 1.28	79.8 ± 2.4	209.7 ± 14.5	−24.6 ± 2.0
2	BuPL-*S*	1.07 ± 0.04	53.4 ± 2.3	32.81 ± 1.51	65.6 ± 3.0	212.4 ± 4.8	−23.9 ± 2.3
3	MuPL-*S*	0.92 ± 0.05	46.0 ± 2.5	36.37 ± 1.30	72.7 ± 2.6	231.5 ± 5.8	−9.9 ± 1.2
4	BMPL-*S*	1.43 ± 0.08	71.3 ± 4.0	28.41 ± 1.73	56.8 ± 3.5	246.1 ± 14.0	−10.3 ± 1.6
5	BMPL-S	1.46 ± 0.07	73.2 ± 3.6	–	–	244.8 ± 9.3	−10.0 ± 1.5
6	MuPL-*S*	–	–	35.71 ± 1.51	71.13	221.6 ± 7.8	−9.7 ± 0.5

Drug loadings, µg/mg of polymer, % EE, encapsulation efficiency. Mean diameter was measured by PCS; ζ (zeta) potentials were quantitated as described in Section 2.

Table 3
Polymer blending, particle size and zeta potential data on blank fluorescein-labeled NPs in uptake studies.

Formula name	Polymer ratio (per weight)				Mean diameter (nm)	Zeta (mV)
	PLA$^{-g\text{-}SEL}$	PLA	Multiblock	PLA$^{-g\text{-}FLU}$		
PL-*F*	–	3	–	1	217.1 ± 4.2	−25.0 ± 3.3
PLS-*F*	2	1	–	1	225.7 ± 6.8	−23.3 ± 2.4
MuPLS-*F*	2	–	1	1	234.9 ± 7.4	−10.6 ± 0.8

qualitative or quantitative experiments, HUVECs were treated with LPS to induce the expression of selectin molecules on their surface [38].

3.4.1. Qualitative studies

Fig. 2 presents a gallery view of HUVEC populations captured by confocal microscopy after 6 or 12 h of incubation with either functionalized (PLS-F) fluorescent NPs (Fig. 2A and B) or control (PL-F) fluorescent NPs (Fig. 2C and D). The overall uptake of functionalized NPs was found to be higher than that of control NPs at both incubation periods. HUVECs treated with the NP vehicle only showed low-level auto-fluorescence not detectable at the settings used to view fluorescent NPs.

To further characterize uptake, single cell views were captured by confocal laser scanning microscopy. Serial z-sections presented fluorescence accumulation inside the cells, not only at the surface (Fig. 2E). The uptake of fluorescent particles by the cells was monitored at different time points. Representative views of 12-h incubation times appear in Fig. 2: 2E depicts the uptake pattern of the functionalized NPs (PLS-F), while, in parallel, the uptake pattern of control fluorescent NPs (PL-F) is displayed in 2F. At 2 h, PLS-Fs were already adherent and integrated in the cell membrane. After 12-h incubation, the cytoplasm appeared to be fully illuminated by the infiltration of NPs and/or their fragments. Moreover, the nucleus seemed to gain at least part of the fluorescence (Fig. 2E). In contrast, the internalization process proceeded at a slower rate for PL-F (control NPs). At 2 h after initiation of the procedure, fluorescent entities could hardly be seen in the vicinity of the cell membrane. At 12 h, fluorescence emitted from the cellular cytoplasm (Fig. 2F) revealed reduced cellular internalization of PL-F compared to PLS-F.

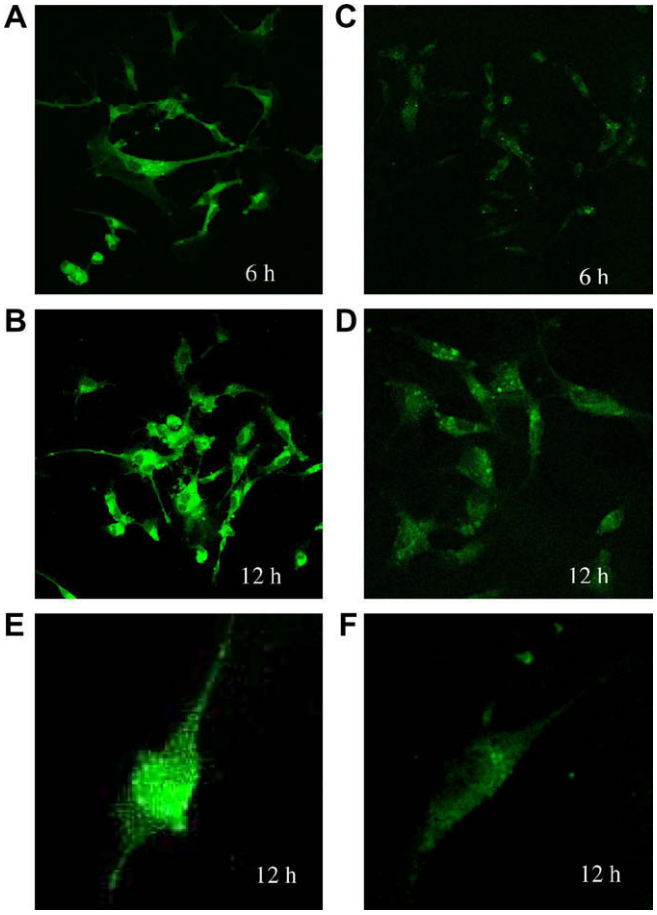

Fig. 2. Gallery-view micrographs as observed by confocal laser scanning microscopy. Images acquired after 6 and 12 h of incubation of activated HUVECs with either functionalized NPs (A and B) or PLA NPs (C and D). Single cell confocal images were acquired after 12-h incubation, with functionalized NPs (E) or PLA control NPs (F).

3.4.2. Quantitative studies

To confirm the above observation, total HUVEC fluorescein content was quantitated at the end of the internalization experiment. After cell lysis, the amount of internalized particles was calculated per μg of cellular protein (Fig. 3). PLS-F uptake was also tested in HUVECs with no LPS pre-treatment to investigate the contributions of selectin overexpression. After 6 h of incubation, cell uptake efficiencies for PLS-F and MuPLS-F were, respectively, 3- and 4.3-fold higher than those for PL-F. In the absence of LPS induction, PLS-F uptake was similar to that of control NPs (PL-F). After 12-h incubation, cell uptake efficiencies of PLS-F and MuPLS-F were, respectively, 3 and 4 times higher than those of PL-F, whereas in the absence of LPS induction, PLS-F uptake was only slightly higher (1.20-fold) than that of PL-F. These results suggest that PLA$^{-g\text{-}SEL}$ in NP production has considerably enhanced their internalization, and, hence, support the confocal microscopy findings.

Interestingly the incorporation of the multiblock co-polymer in the NP matrix (MuPLS-F) induced their enhanced uptake by HUVECs (Fig. 3). It has been reported that increasing matrix hydrophilicity through the incorporation of hydrophilic co-polymer augments the cellular uptake of colloidal particles by the different species of normal and cancerous cells [37,39]. We found that the zeta potential of functionalized NPs dropped from −23.3 to −10.6 mV by incorporation of the PEGylated co-polymer. Hence, a reduced negative surface charge may minimize electrostatic repulsion between the particles and the negatively charged cellular membrane, facilitating particle adhesion to the cell surface with subsequent internalization.

It has been suggested that particle size plays a key role in adhesion to and interaction with living cells [40]. In this respect, NPs in the size range of 100–250 nm can be internalized by endocytosis, while larger particles have to be phagocytosed [41]. The role of selectins (E and/or P) in the functionalized NP uptake has been confirmed by the results obtained without LPS induction (Fig. 3). Indeed, no (after 6 h) or little (after 12 h) uptake improvement was seen for the functionalized NPs versus control NPs. Taken together, since all the tested particles were in the same size range (200–250 nm), these observations suggest that uptake is mainly mediated by a mechanism in which selectin could be involved, perhaps by receptor-mediated endocytosis, as reported for immunoliposomes directed to E-selectin [42].

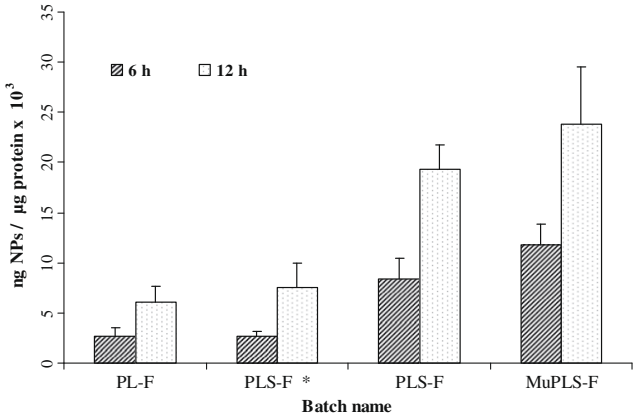

Fig. 3. Effect of NPs on polymer matrix composition and cellular uptake by HUVECs. Incubation times: 6 and 12 h at 37 °C (Data represent the means ± SD, $n = 3$). Details of NP polymer composition are given in Table 3. *Cells not treated by LPS.

3.5. Anti-angiogenic efficacy of free and loaded agents

Having established the activated endothelium-targeting capabilities of these new NPs, both free and drug-loaded NPs were tested for their anti-angiogenic activity in two models. EN and PX efficacy in inhibiting endothelial cell proliferation was assessed in HUVECs *in vitro*. Rat aortic ring assays served as a complete, representative model of angiogenesis. As an organ culture, it is considered to come closest to simulating the *in vivo* situation, as new vessels present all the phases of angiogenesis, from cell proliferation, migration and invasion to tube formation [43]. Combined treatments with NPs were achieved by preparing different batches of NPs co-loaded with different proportions of EN and PX according to the BMPL-*S* formula (Table 2, batches 3, 5 and 6). The NP concentration required to fulfill each scheduled combined treatment was calculated on the basis of the required dose and the loading efficiency of either EN or PX; then, the dose of the other agent was adjusted, whenever necessary, with batch 5 or 6 (Table 2).

3.5.1. HUVEC proliferation assay in the presence of blank or drug-loaded NPs

Although the polymers used for NP preparation were shown not to be toxic, NPs can display specific toxicity because of their size, their accumulation and degradation in cells after internalization or because of the adjuvants included in their preparation [44]. To evaluate the possible toxicity of empty NPs, cell proliferation studies were conducted with NPs produced according to three different formulas for the functionalized NPs (Table 1). The assays showed no influence on HUVEC proliferation in the 0.1–250 µg/ml concentration range for a 3-day incubation time (Fig. 4). Such findings indicate that NP burden will not affect proliferation assay results conducted with drug-loaded NPs for the same incubation time.

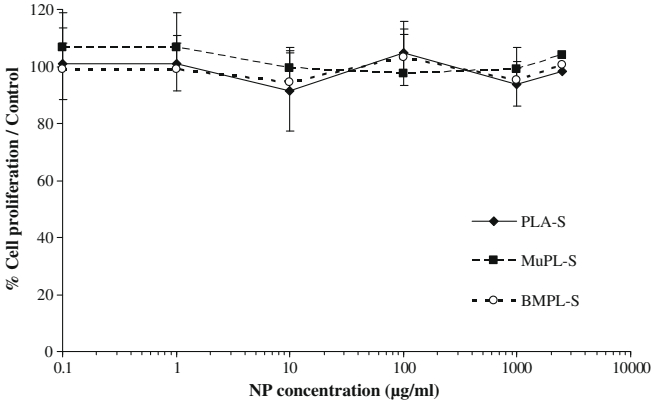

Fig. 4. MTT assay for different formula batches of functionalized NPs in HUVEC culture. NPs were incubated with HUVECs for 72 h before the addition of MTT. Details of NP polymer composition appear in Table 1.

HUVEC proliferation was then followed in response to free drugs or the functionalized NPs loaded with EN or PX or both (Table 2). These experiments were performed on LPS-activated cells. The inhibitory effects of cell proliferation, resulting from the treatments tested, are expressed, as percentage inhibition with reference to control groups (cells treated with drug or NP vehicle only) in each experiment (Table 4).

EN has been reported to block endothelial cycle progression and to reduce the expression of proliferation genes [7]. It induces endothelial cell proliferation [6] and apoptosis pathways in the µg/ml range [45]. In our experiments, we noted 20% proliferation inhibition in response to 1 µg/ml under a 3-day incubation period in immortalized HUVECs, while lower doses (0.25 and 0.5 µg/ml) had no effects. When encapsulated, the 1 µg/ml dose of EN gave about 70% inhibition of proliferation. Even the 0.5 µg/ml dose, when encapsulated, gave significant inhibition (Table 4). Similar observations were made for single PX treatment, as dose-dependent proliferation inhibition was apparent. This anti-proliferative effect was again more pronounced when PX was encapsulated (Table 4), but the difference was mostly seen at the highest concentrations.

Combinations of the two agents displayed a more pronounced inhibitory action than single treatments as either free or loaded NPs. Statistically significant differences were noticeable between all single free and single-loaded drugs except for PX at the lower dose (0.1 µM). Significant differences were also discerned between all free and drug-loaded combinations (Table 4). The inhibitory effect induced by several single-loaded treatments was not significantly different from that evoked by some combinations of the free molecules (see data bearing the superscripts of the same letters in Table 4).

Although surprising (generally encapsulation decreases drug toxicity), it could be explained by protection offered by the nanocarriers against degradation [13,37]. It could also be explained by the contribution of NPs targeting cell membranes, ensuring drug release near the cell surface. Or it could be explained by NP cellular uptake, as reported previously in targeting studies (Section 3.4),

Table 4
Percentage inhibition of enzymatic activity of HUVECs after 72 h incubation with either free or loaded anti-angiogenic agents: endostatin (EN) and/or paclitaxel (PX).

Free EN	Conc. EN	0.25 µg ml^{-1}	0.5 µg ml^{-1}	1 µg ml^{-1}
	% Inhibition	1.75 ± 7.85	11.47 ± 20.56	27.08 ± 5.88^{d}
Free PX	Conc. PX	0.1 µM	1 µM	10 µM
	% Inhibition	26.82 ± 3.61	31.10 ± 5.22	45.04 ± 2.45^{c}
Combination free EN/PX	Conc. EN Conc. PX	0.25 µg ml^{-1}/ 0.01 µM	1 µg ml^{-1}/ 0.1 µM	0.5 µg ml^{-1}/ 1 µM
	% Inhibition	36.14 ± 9.66	51.47 ± 10.98^{b}	65.79 ± 6.39^{a}
Loaded EN	Conc. EN	0.25 µg ml^{-1}	0.5 µg ml^{-1}	1 µg ml^{-1}
	% Inhibition	23.01 ± 5.16	42.38 ± 8.89^{c}	68.67 ± 4.44^{a}
Loaded PX	Conc. PX	0.1 µM	1 µM	10 µM
	% Inhibition	26.96 ± 7.71^{d}	50.92 ± 3.13^{b}	73.97 ± 3.00
Combination loaded EN/PX	Conc. EN Conc. PX	0.25 µg ml^{-1}/ 0.1 µM	1 µg ml^{-1}/ 1 µM	0.5 µg ml^{-1}/ 10 µM
	% Inhibition	46.94 ± 6.18	79.98 ± 2.35	88.06 ± 1.40

Differences between mean values having similar letters as superscripts are not statistically significant at $p < 0.05$.

that could provide on-spot delivery of the drug cargo in targeted cells, increasing their efficacy [46].

It is noteworthy that the doses of NPs, given to HUVECs to obtain the anti-angiogenic drug levels displayed in Table 4, were in the 50–500 μg/ml range (based on load value in Table 2) and were not expected to affect cell proliferation, as illustrated in Fig. 4. Indeed, one of the advantages of co-encapsulation is to decrease NP quantity and thus the polymer burden for the same therapeutic effect.

3.5.2. Rat aortic ring assays: free and single treatment-loaded NPs

Angiogenesis was monitored by the rat aortic ring method with image analysis. Fig. 5 illustrates the different steps of treatment for the tissue culture images obtained. It is important for consistency to ensure the same distance from the aortic ring in the captured culture fields prior to analysis. Hence, images were pre-selected to include a small edge of the aortic artery wall. Vascular density values were computed after the binarization of the treated images (Fig. 5C). For each image, areas showing no vascular growth, such as the aortic wall corner, were excluded from the analysis. The percentage inhibition induced by the tested treatments was calculated with reference to control well data, blank NPs presenting no effect on new vessel sprouting.

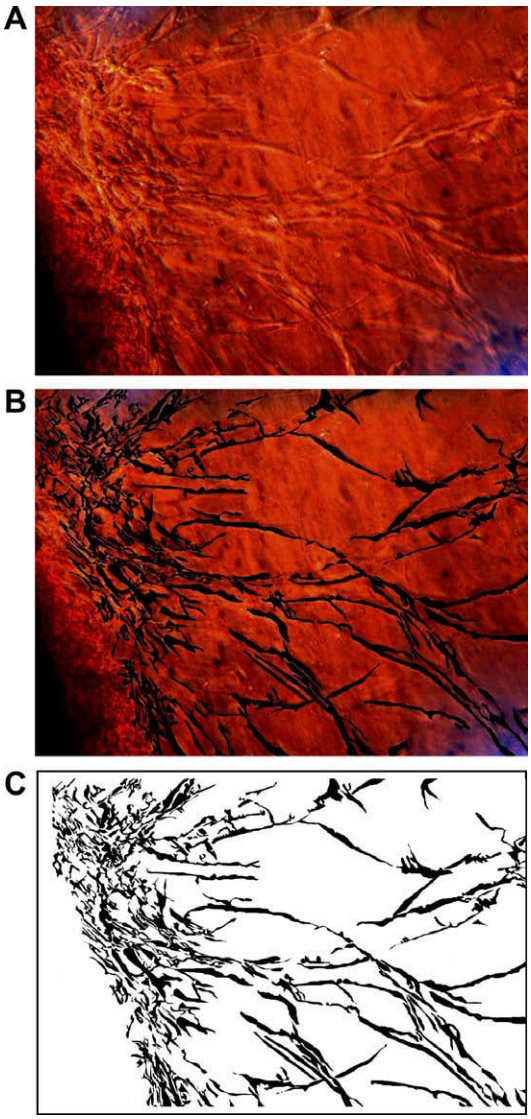

Fig. 5. Processing of a representative picture showing tubular outgrowth from an aortic ring. (A) Raw image of a control culture after 7 days of incubation. (B) Blackening of the emerged tubules. (C) Image binarization. (40×).

Loaded EN was found to be more potent than free EN at the same dose level (Fig. 6), and this outcome was apparent with 7- and 14-day incubation times. Similarly to the results of HUVEC proliferation assays, a significant inhibitory effect of free EN was observed only at the highest concentration tested (1 μg/ml), as no significant action was seen with 0.5 μg/ml. The inhibitory effect increased by 4.5-fold for EN 1 μg/ml in loaded NPs, compared to free drug. A similar, dramatic increment was observed for the 0.5 μg/ml dose, as no inhibition was evidenced when EN was added as a free agent, while a 33% inhibition was documented when EN was added as a NP-loaded agent.

The inhibitory outcome of free and loaded PX at the two concentrations tested was not significantly different after 1 week of treatment. After 2 weeks, however, only the loaded agents manifested persistent action, with the inhibitory values of the free molecules being much lower (F-EN-1, F-PX-1 and F-PX-10). Inhibition values after 7 or 14 days were not significantly different (one-way ANOVA and Fisher's LSD test) for drug-loaded NPs (L-EN-1, L-PX-1 and L-PX-10). These findings support the benefits of microencapsulation to ensure prolonged angiosuppressive activity by either EN or PX. In this respect, it is not surprising to see free EN highly vulnerable to enzymatic degradation by proteases secreted by proliferating tissue, or free PX susceptibility to inactivation by epimerization and hydrolysis during the 2-week study period.

The angiogenesis inhibition levels of PX- and EN-loaded NPs can be explained by the fact that encapsulation protects drugs from degradation and serves as a drug reservoir for sustained release over an extended period of time. NP targeting and cellular uptake were unlikely to contribute to PX and EN activity in this experiment as the NPs were embedded in collagen matrix at the center of the rat aortic ring. The positive effect of PX encapsulation was essentially seen on a long-term basis (14 days), and was consistent, at the same time, with these formulation considerations and with the reported mechanisms of its action [34,47].

3.5.3. Rat aortic ring assays: single and combined treatment-loaded NPs

Fig. 7 depicts the inhibition of angiogenesis induced by the microencapsulated agents either as single treatment or in the form of combined treatment. Sustained angiogenesis inhibition was again observed throughout the study period (7 vs. 14 days) with

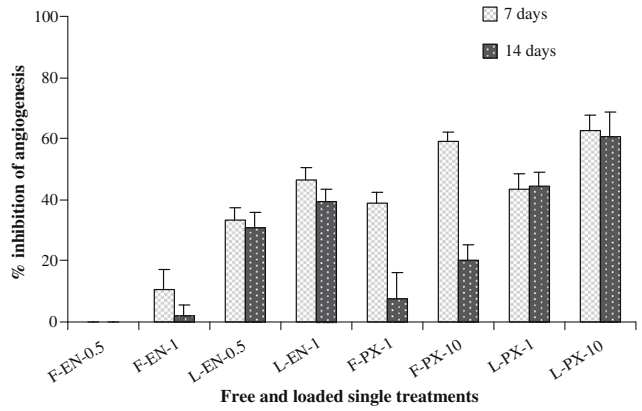

Fig. 6. Inhibition of angiogenesis in rat aortic ring tissue culture in response to free or loaded anti-angiogenic treatment after 7 and 14 days. Endostatin doses. *F-EN-0.5*: 0,5 μg/ml; *F-EN-1*: 1 μg/ml free EN; *L-EN-1*: 1 μg/ml EN-loaded NP; *L-EN-0.5*: 0.5 μg/ml EN-loaded NPs. Paclitaxel doses. *F-PX-10*: 10 μM free PX; *F-PX-1*: 1 μM free PX; *L-PX-10*: 10 μM PX-loaded NP; *L-PX-1*: 1 μM PX-loaded NP (means ± SD, $n = 4$).

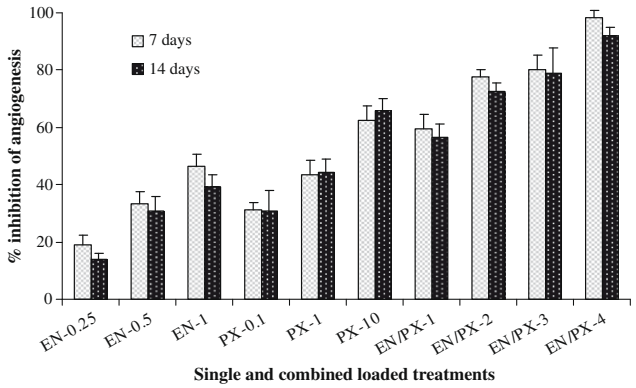

Fig. 7. Inhibition of angiognesis in rat aortic ring tissue culture induced by single and combined anti-angiogenic treatment loaded in functionalized NPs. Single treatment doses: *EN-1*: 1 μg/ml; *EN-0.5*: 0.5 μg/ml; *EN-0.25*: 0.25 μg/ml; *PX-10*: 1 μM; *PX-1*: 1 μM; *PX-0.1*: 0.1 μM. Combined treatment doses: *EN/PX-1*: 0.25 μg/ml/0.1 μM; *EN/PX-2:* 0.5 μg/ml/1 μM; *EN/PX-3*: 0.25 μg/ml/10 μM; *EN/PX-4*: 0.5 μg/ml/10 μM (means ± SD, $n = 4$).

a non-significant difference for all treatments, single or combined (except for EN-1).

It should be noted that EN and PX combination (concentrations of 1 μg/ml and 10 μM, respectively) induced the total inhibition of vascular growth for the entire study period. Indeed, the four combinations presented a powerful inhibitory effect relative to the corresponding concentrations of single treatment with either EN or PX. For example, double treatment, including EN/PX (0.25 μg/ml/0.1 μM), manifested an inhibitory action comparable to 10 μM of PX on day 7 of the experiment, and this inhibitory effect was still maintained after 2 weeks.

Sums of the inhibition values from single drug treatment with either EN or PX were compared statistically (paired *t*-test), with actual inhibition induced by the corresponding combination of both drugs (same doses and incubation times). Co-loading seemed to engender additive effects in most cases (no significant difference between summation and the actual inhibition results obtained with co-loaded drugs). However, with the lower doses of EN and PX (0.25 μg/ml and 0.1 μM, respectively), a statistically significant synergetic outcome was observed at 7 and 14 days (9% and 14% difference in inhibition, respectively). These data could be explained by the anti-angiogenic impact of PX prevailing at low doses, while at higher doses its cytotoxic profile offsets its anti-angiogenic properties. Yet, microencapsulation appears to be important for such an effect to be clearly expressed, either via its targeting or because of continuous release at the action site, ensuring long-term delivery of a constant concentration (reservoir effect) and a constant ratio of the two drugs.

4. Conclusion

The preparation of a new nanoparticular carrier bearing synthetic selectin ligand was optimized. The NPs showed improved uptake by activated HUVECs *in vitro*, and according to the results obtained, we may assume that receptor-mediated endocytosis is one of the mechanisms of internalization. Co-encapsulation of two anti-angiogenic agents was optimized by either microemulsion, incorporation of a hydrophilic multiblock co-polymer, or both techniques. These methods have been shown to adequately enhance the loading of hydrophilic peptides without inducing a considerable decrease in lipophilic drug entrapment. Compared to free drugs, drug-loaded NPs exhibited a powerful and sustained pharmacological action in *in vitro* and *ex vivo* models. Moreover, NPs co-loaded with both EN and PX at lower concentration exhibited a synergetic anti-angiogenic effect. Taken together, the results could be exploited to develop many combined targeted treatments with a variety of anti-angiogenic molecules.

Acknowledgements

The authors thank the Natural Sciences and Engineering Research Council (NSERC) of Canada for financial support, and Dr. Jean-François Bouchard and Anteneh Argaw for their help with confocal microscopy. The editorial work of Mr. Ovid Da Silva on this manuscript is acknowledged.

References

[1] J. Folkman, Tumor angiogenesis: therapeutic implications, N. Engl. J. Med. 285 (21) (1971) 1182–1186.
[2] I. Buysschaert, P. Carmeliet, M. Dewerchin, Clinical and fundamental aspects of angiogenesis and anti-angiogenesis, Acta Clin. Belg. 62 (3) (2007) 162–169.
[3] J. Folkman, Antiangiogenesis in cancer therapy – endostatin and its mechanisms of action, Exp. Cell Res. 312 (5) (2006) 594–607.
[4] J.B. Aragon-Ching, W.L. Dahut, The role of angiogenesis inhibitors in prostate cancer, Cancer J. 14 (1) (2008) 20–25.
[5] C. Folkins, S. Man, P. Xu, Y. Shaked, D.J. Hicklin, R.S. Kerbel, Anticancer therapies combining antiangiogenic and tumor cell cytotoxic effects reduce the tumor stem-like cell fraction in glioma xenograft tumors, Cancer Res. 67 (8) (2007) 3560–3564.
[6] M.S. O'Reilly, T. Boehm, Y. Shing, N. Fukai, G. Vasios, W.S. Lane, E. Flynn, J.R. Birkhead, B.R. Olsen, J. Folkman, Endostatin: an endogenous inhibitor of angiogenesis and tumor growth, Cell 88 (2) (1997) 277–285.
[7] A. Abdollahi, P. Hahnfeldt, C. Maercker, H.J. Grone, J. Debus, W. Ansorge, J. Folkman, L. Hlatky, P.E. Huber, Endostatin's antiangiogenic signaling network, Mol. Cell 13 (5) (2004) 649–663.
[8] A. Abdollahi, L. Hlatky, P.E. Huber, Endostatin: the logic of antiangiogenic therapy, Drug Resist. Updat. 8 (1–2) (2005) 59–74.
[9] O. Kisker, C.M. Becker, D. Prox, M. Fannon, R. D'Amato, E. Flynn, W.E. Fogler, B.K. Sim, E.N. Allred, S.R. Pirie-Shepherd, J. Folkman, Continuous administration of endostatin by intraperitoneally implanted osmotic pump improves the efficacy and potency of therapy in a mouse xenograft tumor model, Cancer Res. 61 (20) (2001) 7669–7674.
[10] W.T. Loo, J.H. Fong, M.N. Cheung, L.W. Chow, The efficacy of Paclitaxel on solid tumour analysed by ATP bioluminescence assay and VEGF expression: a translational research study, Biomed. Pharmacother. 59 (Suppl. 2) (2005) S337–S339.
[11] B. Lennernas, P. Albertsson, H. Lennernas, K. Norrby, Chemotherapy and antiangiogenesis – drug-specific, dose-related effects, Acta Oncol. 42 (4) (2003) 294–303.
[12] M. Xie, L. Zhou, T. Hu, M. Yao, Intratumoral delivery of paclitaxel-loaded poly(lactic-co-glycolic acid) microspheres for Hep-2 laryngeal squamous cell carcinoma xenografts, Anticancer Drugs 18 (4) (2007) 459–466.
[13] T. Musumeci, L. Vicari, C.A. Ventura, M. Gulisano, R. Pignatello, G. Puglisi, Lyoprotected nanosphere formulations for paclitaxel controlled delivery, J. Nanosci. Nanotechnol. 6 (9–10) (2006) 3118–3125.
[14] L. Mu, S.S. Feng, Vitamin E TPGS used as emulsifier in the solvent evaporation/extraction technique for fabrication of polymeric nanospheres for controlled release of paclitaxel (Taxol), J. Control. Release 80 (1–3) (2002) 129–144.
[15] J.M. Kuldo, K.I. Ogawara, N. Werner, S.A. Asgeirsdottir, J.A. Kamps, R.J. Kok, G. Molema, Molecular pathways of endothelial cell activation for (targeted) pharmacological intervention of chronic inflammatory diseases, Curr. Vasc. Pharmacol. 3 (1) (2005) 11–39.
[16] C. Kneuer, C. Ehrhardt, M.W. Radomski, U. Bakowsky, Selectins – potential pharmacological targets?, Drug Discov Today 11 (21–22) (2006) 1034–1040.
[17] V. Nadeau, G. Leclair, S. Sant, J.M. Rabanel, R. Quesnel, P. Hildgen, Synthesis of new versatile functionalized polyesters for biomedical applications, Polymer 46 (25) (2005) 11263–11272.
[18] M. Hombreiro Perez, C. Zinutti, A. Lamprecht, N. Ubrich, A. Astier, M. Hoffman, R. Bodmeier, P. Maincent, The preparation and evaluation of poly(epsilon-caprolactone) microparticles containing both a lipophilic and a hydrophilic drug, J. Control. Release 65 (3) (2000) 429–438.
[19] T. Hammady, A. El-Gindy, E. Lejmi, R.S. Dhanikula, P. Hildgen. Characteristics and properties of nanospheres co-loaded with lipophilic and hydrophilic drug models. Int. J. Pharm., in press.
[20] E.E. Simanek, G.J. McGarvey, J.A. Jablonowski, C.H. Wong, Selectin–carbohydrate interactions: from natural ligands to designed mimics, Chem. Rev. 98 (1998) 833–862.
[21] X. Banquy, G. Leclair, J.M. Rabanel, A. Argaw, J.F. Bouchard, P. Hildgen, S. Giasson, Selectins ligand decorated drug carriers for activated endothelial cell targeting, Bioconj. Chem. 19 (10) (2008) 2030–2039.
[22] R. Quesnel, P. Hildgen, Synthesis of PLA-b-PEG multiblock copolymers for stealth drug carrier preparation, Molecules 10 (1) (2005) 98–104.
[23] T. Mossman, Rapid colorimetric assay for cellular growth and survival – application to proliferation and cyto-toxicity assays, J. Immunol. Methods 65 (1–2) (1983) 55–63.

[24] A. Lamprecht, N. Ubrich, M. Hombreiro Perez, C. Lehr, M. Hoffman, P. Maincent, Influences of process parameters on nanoparticle preparation performed by a double emulsion pressure homogenization technique, Int. J. Pharm. 196 (2) (2000) 177–182.
[25] T. Hammady, V. Nadeau, P. Hildgen, Microemulsion and diafiltration approaches: an attempt to maximize the global yield of DNA-loaded nanospheres, Eur. J. Pharm. Biopharm. 62 (2) (2006) 143–154.
[26] D. Girardot, B. Jover, J.P. Moles, D. Deblois, P. Moreau, Chronic nitric oxide synthase inhibition prevents new coronary capillary generation, J. Cardiovasc. Pharmacol. 44 (3) (2004) 322–328.
[27] T. Elsdale, J. Bard, Collagen substrata for studies on cell behavior, J. Cell Biol. 54 (3) (1972) 626–637.
[28] R. Wild, S. Ramakrishnan, J. Sedgewick, A.W. Griffioen, Quantitative assessment of angiogenesis and tumor vessel architecture by computer-assisted digital image analysis: effects of VEGF-toxin conjugate on tumor microvessel density, Microvasc. Res. 59 (3) (2000) 368–376.
[29] S. Sant, S. Poulin, P. Hildgen, Effect of polymer architecture on surface properties, plasma protein adsorption, and cellular interactions of pegylated nanoparticles, J. Biomed. Mater. Res. A 87A (4) (2008) 885–895.
[30] A. Sanchez, M. Tobio, L. Gonzalez, A. Fabra, M.J. Alonso, Biodegradable micro- and nanoparticles as long-term delivery vehicles for interferon-alpha, Eur. J. Pharm. Sci. 18 (3–4) (2003) 221–229.
[31] J. Rojas, H. Pinto-Alphandary, E. Leo, S. Pecquet, P. Couvreur, A. Gulik, E. Fattal, A polysorbate-based non-ionic surfactant can modulate loading and release of beta-lactoglobulin entrapped in multiphase poly(DL-lactide-co-glycolide) microspheres, Pharm. Res. 16 (2) (1999) 255–260.
[32] R. Audran, Y. Men, P. Johansen, B. Gander, G. Corradin, Enhanced immunogenicity of microencapsulated tetanus toxoid with stabilizing agents, Pharm. Res. 15 (7) (1998) 1111–1116.
[33] T. Hammady, R. Singh, A. El-Gindy, E. Lejmi, P. Moreau, P. Hildgen. Characterization and assessment of biological activity of nanospheres loaded with all *trans*-retinoic acid and DNA, in AAPS Annual Meeting and Exposition, 2005.
[34] C. Fonseca, S. Simoes, R. Gaspar, Paclitaxel-loaded PLGA nanoparticles: preparation, physicochemical characterization and in vitro anti-tumoral activity, J. Control. Release 83 (2) (2002) 273–286.
[35] B.B. Youan, A. Hussain, N.T. Nguyen, Evaluation of sucrose esters as alternative surfactants in microencapsulation of proteins by the solvent evaporation method, AAPS PharmSci. 5 (2) (2003) E22.
[36] S. Nema, R.J. Washkuhn, R.J. Brendel, Excipients and their use in injectable products, PDA J. Pharm. Sci. Technol. 51 (4) (1997) 166–171.
[37] Z. Zhang, S.S. Feng, The drug encapsulation efficiency, in vitro drug release, cellular uptake and cytotoxicity of paclitaxel-loaded poly(lactide)-tocopheryl polyethylene glycol succinate nanoparticles, Biomaterials 27 (21) (2006) 4025–4033.
[38] M. Colden-Stanfield, E.K. Gallin, Modulation of K^+ currents in monocytes by VCAM-1 and E-selectin on activated human endothelium, Am. J. Physiol. 275 (1 Pt 1) (1998) C267–C277.
[39] T. Jung, W. Kamm, A. Breitenbach, E. Kaiserling, J.X. Xiao, T. Kissel, Biodegradable nanoparticles for oral delivery of peptides: is there a role for polymers to affect mucosal uptake?, Eur J. Pharm. Biopharm. 50 (1) (2000) 147–160.
[40] K.Y. Win, S.S. Feng, Effects of particle size and surface coating on cellular uptake of polymeric nanoparticles for oral delivery of anticancer drugs, Biomaterials 26 (15) (2005) 2713–2722.
[41] K.A. Foster, M. Yazdanian, K.L. Audus, Microparticulate uptake mechanisms of in-vitro cell culture models of the respiratory epithelium, J. Pharm. Pharmacol. 53 (1) (2001) 57–66.
[42] S. Kessner, A. Krause, U. Rothe, G. Bendas, Investigation of the cellular uptake of E-Selectin-targeted immunoliposomes by activated human endothelial cells, Biochim. Biophys. Acta 1514 (2) (2001) 177–190.
[43] R. Auerbach, R. Lewis, B. Shinners, L. Kubai, N. Akhtar, Angiogenesis assays: a critical overview, Clin. Chem. 49 (1) (2003) 32–40.
[44] K.R. Vega-Villa, J.K. Takemoto, J.A. Yanez, C.M. Remsberg, M.L. Forrest, N.M. Davies, Clinical toxicities of nanocarrier systems, Adv. Drug Deliv. Rev. 60 (8) (2008) 929–938.
[45] M. Dhanabal, R. Ramchandran, M.J. Waterman, H. Lu, B. Knebelmann, M. Segal, V.P. Sukhatme, Endostatin induces endothelial cell apoptosis, J. Biol. Chem. 274 (17) (1999) 11721–11726.
[46] C.S. Cho, K.Y. Cho, I.K. Park, S.H. Kim, T. Sasagawa, M. Uchiyama, T. Akaike, Receptor-mediated delivery of all *trans*-retinoic acid to hepatocyte using poly(L-lactic acid) nanoparticles coated with galactose-carrying polystyrene, J. Control. Release 77 (1–2) (2001) 7–15.
[47] D.S. Grant, T.L. Williams, M. Zahaczewsky, A.P. Dicker, Comparison of antiangiogenic activities using paclitaxel (taxol) and docetaxel (taxotere), Int. J. Cancer 104 (1) (2003) 121–129.